Computational Study of the Geometry and Properties of the Metcars Ti_8C_{12} and Mo_8C_{12}

Hua Hou,*,† James T. Muckerman,* Ping Liu, and José A. Rodriguez

Chemistry Department, Brookhaven National Laboratory, Upton, New York 11973-5000

Received: June 24, 2003

We report the results of extensive ab initio HF and post-HF (as well as DFT) studies of the "magic number" metallocarbohedrene ("metcar") clusters Ti_8C_{12} and Mo_8C_{12} in various electronic states of T_d symmetry and the Jahn−Teller-distorted D_{2d}, C_{3v}, and C_1 symmetries. An essential feature of the present work is that it is a systematic study employing a hierarchy of theoretical methods to explore the effect of refining the treatment of electron correlation in determining the geometry and electronic ground state of these species. For Ti_8C_{12}, we show using relatively high-level theories such as MP2, MP4, and QCISD that the Aufbau principle for the occupation of the molecular orbitals is obeyed, resulting in a Jahn−Teller distortion of the proposed T_d symmetry. These higher-level calculations identify a D_{2d} structure close to T_d symmetry for the electronic ground state and allow some of its chemical properties to be explored with confidence using a lower level of theory. The reactivity of Ti_8C_{12} toward H_2O, CO, and Cl is also investigated. It is found that Ti_8C_{12} can act as a Lewis acid to accept lone pairs of electrons from H_2O (Lewis base) and that it can also be oxidized by Cl atoms through electron donation from C_2 units in Ti_8C_{12} to the Cl mediated by a Ti d_{z^2} orbital. Thus, a relationship among structure, electronic properties, and reactivity is established. For Mo_8C_{12}, we find that the T_d structure is not subject to a Jahn−Teller effect, and it is a true minimum at the HF level; B3LYP DFT calculations prefer a lower-symmetry (near-D_2) structure. The results of ab initio and DFT methods are compared.

I. Introduction

Castleman and co-workers discovered the "magic number" Ti_8C_{12} cluster in 1992.[1−3] Since that time, much work, both experimental[4−13] and theoretical,[14−31] has focused on this molecule and its reactivity toward other molecules. However, the detailed geometric structure and even the ground electronic state of this molecule are still unresolved issues.

A pentagonal dodecahedron structure corresponding to T_h symmetry, as shown in Figure 1, was originally proposed by Castleman and co-workers by analogy with the hypothetical C_{20} fullerene.[1−3] Subsequent DFT calculations, especially those by Dance,[16,23] made a strong case for a tetrahedral structure (T_d symmetry) in which an outer tetrahedron of Ti atoms (denoted THN) is connected through σ-bonded C_2 units and an (inverted) inner tetrahedron of Ti atoms (denoted "thn"), each of which is η^2-bonded to three of the C_2 units, to the three other Ti atoms of the inner tetrahedron, and to three of the Ti atoms of the outer tetrahedron. This T_d structure (similar to the second structure shown in Figure 1) contains a total of 60 chemical bonds of which 36 are Ti−C bonds.

Rohmer et al. extensively examined seven topologically distinct minima corresponding to T_d, D_2, D_{2d}, C_{2v}, two types of D_{3d}, and C_s symmetries on the Ti_8C_{12} potential energy surface using Hartree−Fock (HF) and configuration-interaction (CI) methods.[18,21,26] All of these seven minima share two common characteristics: (1) they all can be described as distorted cubes of metal atoms with a C_2 unit capping each face along one diagonal and (2) they have a total of 36 Ti−C chemical bonds. As first proposed by Dance,[16,23] they found the T_d structure described above to be the most stable geometric structure for Ti_8C_{12}. Their ab initio calculations at the HF level favored a "$^5A_2$" ground state in which the four unpaired electrons occupied the $4a_1$ and the three components of the $7t_2$ orbital. Herein we refer to this state as $^5A_1(7t_2)$. The four singly occupied orbitals in this state all correspond to the d_{z^2} orbitals on Ti atoms of the inner tetrahedron. However, an eight-configuration state involving the same four electrons and orbitals with "singlet coupling of the four unpaired metal electrons" was found to be lower in energy than the quintet state. CI calculations involving the highest 20 (metal) electrons further indicated that this multiconfiguration singlet state is the lowest-energy state in T_d symmetry. They asserted that the "proper localization of the d metal electrons rather than the Aufbau principle is defined as the decisive criterion for selecting the ground-state electronic configuration."[21]

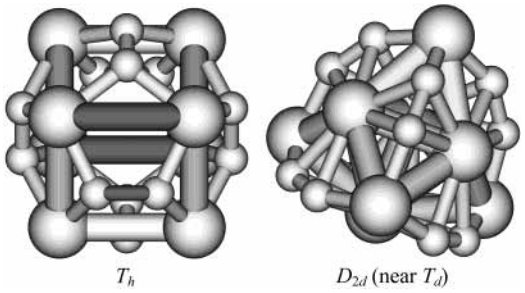

Figure 1. Optimal geometric structures for Ti_8C_{12} in T_h (left) and D_{2d}, near-T_d, symmetry (right) from HF calculations with the 6-31G(d) basis. The larger spheres are Ti atoms, and the smaller spheres, C atoms.

There were, however, some important issues that were ignored in the previous work regarding the most preferred T_d structure: (1) In Rohmer et al.'s CI calculations,[18,21] the correlation of only a relatively small number of electrons (the 20 "metal" electrons) was taken into account. It is not clear if this treatment

* Corresponding authors. E-mail: muckerma@bnl.gov. E-mail: houhua@chem.whu.edu.cn.

† Present address: College of Chemistry and Molecular Sciences, Wuhan University, Wuhan 430072, P. R. China.

10.1021/jp0357976 CCC: $25.00
Published on Web 10/11/2003

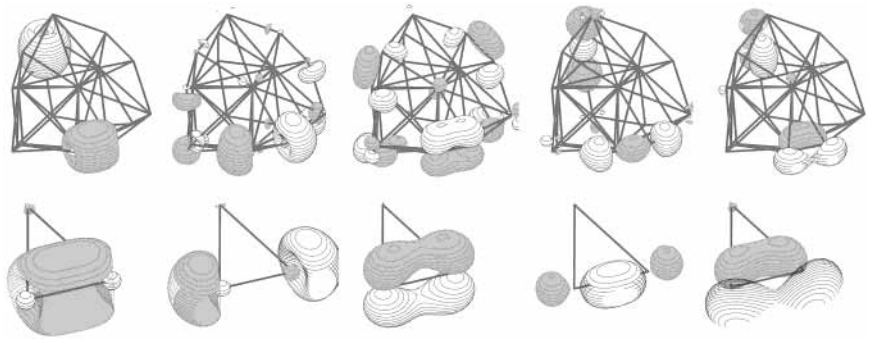

Figure 2. Valence orbitals of Ti_8C_{12} and TiC_2. The upper orbitals are the first 30 occupied valance orbitals of Ti_8C_{12} (groups of 6 orbitals for each of the 5 types shown). The lower orbitals are the first 5 occupied valance orbitals of TiC_2. These orbitals are all related to the C−C bonds: σ(s), σ^*(s), $\pi(p_x)$, $\sigma(p_z)$, and $\pi(p_y)$.

of the correlation is sufficient. Would the results be significantly changed if all of the valence electrons were correlated? (2) The Aufbau principle for the electron occupancy of the molecular orbitals would place the last two electrons in a triply degenerate ($4t_1$) orbital, leading to a first-order Jahn−Teller effect and the distortion of the T_d symmetry to a lower symmetry such as C_{3v} or D_{2d}. (Note that this D_{2d} structure is quite different from the one considered by Rohmer et al. mentioned above.[21] This one, shown in Figure 1, is only slightly distorted from T_d symmetry, and we refer to it as D_{2d} (near-T_d)). There has been some work exploring lower-symmetry structures arising from the Jahn−Teller effect in Ti_8C_{12}.[18,29−31] However, these studies employed either DFT or SCF-HF calculations. There have been no high-level ab initio (post-HF) calculations addressing the detailed geometries and properties of lower-symmetry structures.

In this article, we report the results of extensive ab initio HF and post-HF, as well as density functional (DF), studies of the Ti_8C_{12} cluster in various states in T_d symmetry and the Jahn−Teller distorted D_{2d}, C_{3v}, and C_1 symmetries. An essential feature of the present work is that we have explored the effect of full-valence electron correlation (and in some cases, all-electron correlation) versus only 20-electron correlation using high-level theories such as MP2, MP4, and QCISD. Contrary to the conclusion of the previous work,[21] we find that the Aufbau principle for the occupation of the molecular orbitals is obeyed. The electronic properties and reactivity of Ti_8C_{12} are also investigated, and the relationship between them is interpreted.

The $Mo_8C_{12}^+$ ion was determined to be a magic number cluster by Pilgrim and Duncan,[32] and the neutral Mo_8C_{12} cluster has also recently been observed experimentally to be a magic number species.[33] Theoretically, Lin and Hall studied this cluster at the HF level and found that it has the magic metal electron number (36) according to their calculated orbital interaction scheme for a tetracapped tetrahedral metal cluster with T_d symmetry.[34] To the best of our knowledge, there is no other previous theoretical study of this cluster and no previous study elucidating the details of its electronic properties (vibrational frequencies, atomic charges, orbitals, etc.). Would Mo_8C_{12} be similar to Ti_8C_{12} in its structure and properties? In the present work, we optimized the geometry and calculated the vibrational frequencies of Mo_8C_{12} at both the HF and B3LYP DFT levels of theory. Some of its electronic properties were also investigated.

DFT methods are widely used to study larger systems because they are fast compared to expensive high-level ab initio methods yet include electron correlation effects. However, DFT methods, which employ empirical functionals, are not favored for accurate calculations on small molecules. We cannot necessarily assume that all of the results of DFT calculations are accurate without further tests. From a theoretical point of view, Ti_8C_{12} is a molecule of convenient size to serve as a test bed for comparing the results of ab initio and DFT methods. In this work, we have carried out such a comparison.

II. Geometric Structure and Energetics of Ti_8C_{12}

The 6-31G(d) basis[35,36] was adopted as the standard basis in which all levels of calculation were carried out. Additional calculations were performed with larger basis sets as well as with pseudopotential basis sets for the metal atoms to explore convergence issues. All calculations were performed with the Gaussian 98[37] and MOLPRO 2002[38] program packages.

***T_d* Symmetry.** As discussed in the Introduction, the tetra-capped tetrahedron structure with T_d symmetry was proposed to be the preferred structure for Ti_8C_{12}. In this structure, the eight Ti atoms are grouped into two sets: four equivalent capping Ti atoms (THN) and another four equivalent capped Ti atoms (thn). The six C_2 units are equivalent and aligned along the capping (outer) Ti−Ti diagonals (Figure 1).

To understand well the various states of interest in T_d symmetry, we first need to understand the valence orbitals to obtain a clear picture of the electron occupation pattern. There is a total of 80 valence electrons. Interestingly, the first 30 valence orbitals (accommodating 60 electrons) are all associated with the 6 C_2 units in Ti_8C_{12}. These 30 orbitals fall into 5 groups of 6 orbitals corresponding to each of the first 5 N_2-like occupied valence orbitals of the building block fragment TiC_2, which has an equilibrium structure of C_{2v} symmetry (Figure 2).[39] Then, 16 of the remaining 20 electrons take part in π-back-donation interactions between Ti atoms and the C−C π^* orbitals. These first 38 valence orbitals were found scarcely to change from one state to another. Where do the last four electrons go? What kinds of orbitals on which sets of Ti atoms (THN or thn) do they occupy? Are they paired into two orbitals, or are they unpaired? This is the key and difficult issue in determining the electronic ground state and the most energetically favorable geometry. Because there are several ways to place these last four electrons, to understand them well we first examined the low-lying unoccupied orbitals of the ions $Ti_8C_{12}^{4+}$ and $Ti_8C_{12}^{2+}$.

Figure 3 shows the orbital-energy diagrams for the ground $^1A_1$ states of the $Ti_8C_{12}^{4+}$ and $Ti_8C_{12}^{2+}$ ions at their optimal geometries at the HF/6-31G(d) level of theory. The highest eight doubly occupied orbitals of the $Ti_8C_{12}^{4+}$ ion (Figure 3a), the components of 4e, $3t_1$, and $6t_2$, are Ti d orbitals interacting with the C−C π^* orbitals as mentioned above. The $4a_1$ orbital is the in-phase combination of four d_{z^2} orbitals on the inner Ti atoms. The triply degenerate $4t_1$ orbital, more like the orbitals 4e, $3t_1$, and $6t_2$, has the character of the d orbitals of the four outer Ti

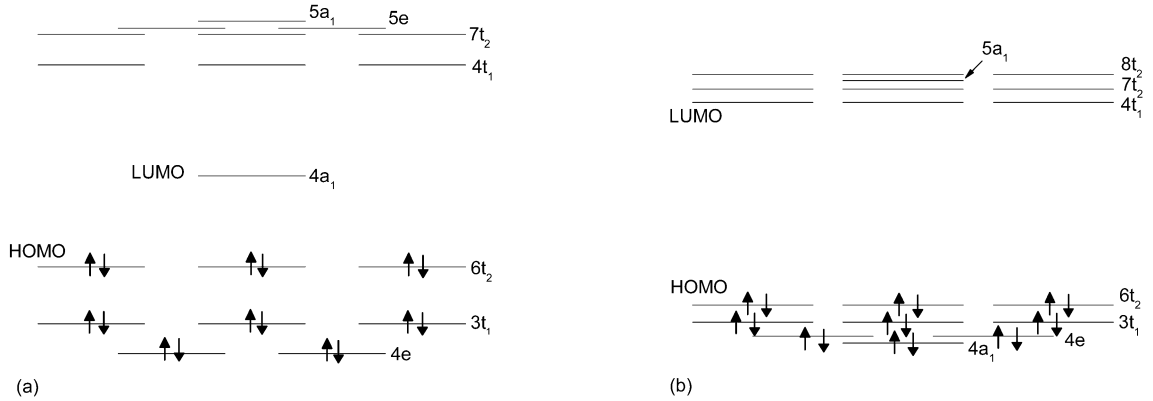

Figure 3. Frontier orbitals of the $Ti_8C_{12}^{4+}$ (a) and $Ti_8C_{12}^{2+}$ (b) ions in T_d symmetry optimized at the HF/6-31G(d) level of theory.

TABLE 1: Absolute (in hartree) and Relative Energies (in kcal/mol) of Various States of Ti_8C_{12} in T_d Symmetry Calculated with Different High-Level ab Initio Theories[a] with the 6-31G(d) Basis

method\state	$^5A_1(7t_2)$	MC $^1A_1$	MC $^3T_1$	$^5A_1(4t_1)$	$^1A_1(5a_1)$	cusp 1	cusp 2	absolute energies[b]
HF (optimal)	8.4			154.2	134.5	115.8	121.4	−7240.899232
CASSCF(4,4)		**0.0**[c]	2.9[c]					−7240.912592
CISD [20e]	12.5	**0.0**[d]	4.0[d]	121.6	86.5	72.4	68.9	−7241.298730
MP2 [80e]	131.4			75.5	31.3	14.8	**0.0**	−7244.052575
MP2 [248e]	166.7	160.8[e]		85.7	40.1	20.0	**0.0**	−7245.834235
MP4(SDQ) [80e]					34.4	**0.0**	22.8	−7243.969200
QCISD [80e]					17.5	**0.0**	13.2	−7243.577956
MP2 optimal [80e]					39.1	11.0	**0.0**	−7244.088001

[a] State energies relative to the lowest-energy state at each level of theory. [b] Absolute energies for the lowest state at each level of theory. [c] Optimal geometry of the $^5A_1(7t_2)$ state. [d] MRCI result. [e] CASMP2 result.

atoms interacting with C−C π^* orbitals. The other low-lying triply degenerate orbital, $7t_2$, is composed of three differently phased combinations of d_{z^2} orbitals on the inner Ti atoms as in $4a_1$.

On the basis of the orbital energy diagram for $Ti_8C_{12}^{4+}$, we can obtain the following possible configurations for the ground electronic state of neutral Ti_8C_{12} in T_d symmetry: (1) the metal-localized quintet state $^5A_1(7t_2)$ generated by placing the four electrons into the $4a_1$ and $7t_2$ orbitals; (2) the multiconfiguration MC $^1A_1$ state corresponding to the "singlet coupling" of the four electrons in the $4a_1$ and $7t_2$ orbitals; and (3) the metal-delocalized $^5A_1(4t_1)$ state formed by placing the four electrons into $4a_1$ and the triply degenerate $4t_1$ orbital because $4t_1$ is slightly lower in energy than $7t_2$.

The $4a_1$ orbital should tend to be doubly occupied given the fact that there is a large energy gap between $4a_1$ and $4t_1$ (1.6 eV). Indeed, in the orbital energy diagram for the $Ti_8C_{12}^{2+}$ ion (Figure 3b), the doubly occupied $4a_1$ orbital is seen to be greatly stabilized and becomes the lowest of the metal d orbitals involved in the bonding. How can the last two electrons be placed to obtain closed-shell neutral Ti_8C_{12} configurations that compete to be the principle configuration(s) of the lowest singlet state? This is the crux of the problem. The Aufbau principle would place these two electrons into the triply degenerate $4t_1$ orbital. This would lead to a first-order Jahn−Teller effect and the distortion of T_d symmetry to some lower symmetry. There is also the possibility of low-lying symmetry-breaking triplet states (vide infra). To explore the Jahn−Teller effect within the T_d nuclear framework, we investigated two closed-shell "cusp" states with symmetry-breaking wave functions arising from the inequivalent population of the components of a triply degenerate orbital: (1) cusp 1 with configuration $(4a_1)^2(4e)^4(3t_1)^6(6t_2)^6(4t_1)^2$ that is related to the above-mentioned $^5A_1(4t_1)$ state and (2) cusp 2 with configuration $(4a_1)^2(4e)^4(3t_1)^6(6t_2)^6(7t_2)^2$ that is related to the open-shell state $^5A_1(7t_2)$. The true Jahn−Teller cusp state would be the degenerate state at a conical intersection with a symmetry-preserving wave function,[40] but such a state cannot be expressed as a single determinant. The cusp states considered here are thus already stabilized by the purely electronic component of the Jahn−Teller effect. What remains to be determined is the additional stabilization arising from the geometric distortion from T_d symmetry. Note that in a symmetry-constrained geometry optimization this type of cusp state never converges with respect to force but does converge with respect to energy and displacement. Here we use the term "state" loosely to denote the result of a single-configuration HF or the lowest root of a single-reference CI calculation. Such so-called states thus represent different approximations to the lowest eigenstate of the Hamiltonian operator for the system. These are not distinct molecular states unless they correspond to *different* roots of the *same* Hamiltonian matrix.

To avoid a Jahn−Teller distortion of the T_d symmetry, the last two electrons could occupy the higher-energy $5a_1$ orbital, which is composed of the d_{z^2} orbitals on the four outer Ti atoms. This generates another closed-shell singlet state that we label $^1A_1(5a_1)$.

As can be seen from Table 1, $^5A_1(7t_2)$ is the lowest-energy state of T_d symmetry at the (in all cases restricted) HF level of theory. However, the MC $^1A_1$ state from a CASSCF(4,4) calculation in which the four unpaired electrons in the $^5A_1(7t_2)$ state are singlet coupled is lower in energy. At the CISD level with 20 electrons correlated, the MC $^1A_1$ state is lower than $^5A_1(7t_2)$ by 12.5 kcal/mol. There is also a "triplet coupling" MC $^3T_1$ state that lies 4.0 kcal/mol above the MC $^1A_1$ state at the CISD level of theory with 20 active electrons. All of the other states, including the two cusp states, are much higher in energy than these $^5A_1(7t_2)$, MC $^1A_1$, and MC $^3T_1$ states at this level of theory. This aspect of our results is entirely consistent with the results of Rohmer and co-workers[18,21] and represents a confirmation of their results using a larger basis. However, we interpret the MC $^1A_1$ state somewhat differently than in the previous work. In the work of Rohmer et al.,[21] it was referred

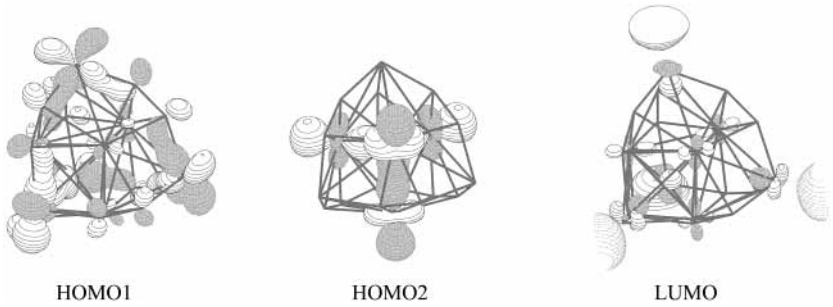

Figure 4. Orbital plots of the HOMO (both alternatives, HOMO1 and HOMO2) and LUMO in D_{2d} symmetry obtained at the HF/6-31G(d) level of theory.

to as the singlet-coupled analogue of the $^5A_1(7t_2)$ state; however, we see it primarily as a spatially averaged closed-shell state even though it has some open-shell character. (There are no important configurations with only one doubly occupied orbital.) The two-configuration singlet state in which the four electrons are restricted to occupy the four different orbitals that are singly occupied in the $^5A_1(7t_2)$ state (i.e., the four electrons are unpaired but singlet-coupled) has an energy higher than the CASSCF-(4,4) MC $^1A_1$ state by 367.9 kcal/mol. Furthermore, multireference configuration interaction (MRCI) calculations with 20 active (metal) electrons based on the 2- and 8-configuration singlet reference functions place the completely open-shell singlet state 236.7 kcal/mol above the MC $^1A_1$ state. These facts lead us to question Rohmer et al.'s "high-spin" characterization of the MC $^1A_1$ state.

We now turn to the question of how this picture of the state energies in T_d symmetry is modified by considering a higher level of electron correlation. At the MP2 level with all 248 electrons correlated, it can be seen in Table 1 that the results change dramatically. The two cusp states (cusp 1 and cusp 2) become the lowest ones, and the closed-shell $^1A_1(5a_1)$ state is the next most stable state, followed by the $^5A_1(4t_1)$ state. The CASMP2 result for the MC $^1A_1$ state lies even higher and is not the lowest-energy symmetry-conserving singlet state in T_d geometry; the $^1A_1(5a_1)$ state is. It is clear from Table 1 that correlating all 80 valence electrons (or all 248 electrons) gives a very different result than correlating only 20 (metal) electrons. The correlation of the inner-valence electrons tends to act in opposition to the effect of correlating only the 20 outer-valence electrons, and correlating core electrons enhances this effect. We will discuss this issue in more detail below.

It is also evident from Table 1 that the two cusp states (cusp 1 and cusp 2) are lower than the closed-shell $^1A_1(5a_1)$ state at all levels of theory used. To strengthen this point, we reoptimized the geometry of these three states at the MP2(80e)/6-31G(d) level. The energy differences between the $^1A_1(5a_1)$ and the two cusp states are 28.1 and 39.1 kcal/mol at the MP2-optimized geometries. These results clearly indicate that because of the first-order Jahn−Teller effect the most stable structure is not of T_d symmetry. The Jahn−Teller distortion to some lower symmetry will lower the system's energy.

Jahn−Teller Distortion: D_{2d}, C_{3v} and C_1 Symmetry. Rohmer et al. considered a $^1A_1$ state in D_{2d} symmetry at the HF level of theory, but because its energy was higher than that of their calculated $^5A_1(7t_2)$ state, they concluded that high-spin highly symmetric structures were preferred over low-spin Jahn−Teller distorted ones.[18] Here we consider two symmetry-constrained distortion paths from T_d symmetry. One leads to structures of D_{2d} symmetry by elongating or compressing the T_d-symmetry framework along one of the C_2 axes. In D_{2d} symmetry, the six C_2 units are split into two sets: one set with four equivalent C_2 units and the other with two equivalent C_2 units. For the eight Ti atoms, as in T_d symmetry, the four outer capping Ti atoms remain equivalent, as do the four inner capped Ti atoms. Another distortion path leads to structures of C_{3v} symmetry by elongating or compressing the T_d framework along one C_3 axis. In C_{3v} symmetry, the six C_2 units are also split into two sets, but with three C_2 units in each set. The four Ti atoms of each tetrahedron are split into two groups of three and one.

Interestingly, there are two possible electronic configurations in each reduced symmetry structure with the major difference between them being the highest occupied molecular orbital (HOMO). This arises from a competition between the two cusp states, cusp 1 and cusp 2. We label these two different HOMOs as HOMO1 and HOMO2 corresponding to cusp 1 and cusp 2, respectively. HOMO1 consists of d_{xz}-like orbitals on the four outer Ti atoms interacting with C−C π^* orbitals, whereas HOMO2 is composed of d_{z^2}-like orbitals on the four inner Ti atoms. When T_d symmetry is lowered to D_{2d} or C_{3v} symmetry, HOMO1 ($4t_1$) splits into the $9a_2$ and 32e orbitals in D_{2d} symmetry and the $9a_2$ and 41e orbitals in C_{3v} symmetry; HOMO2 ($7t_2$) becomes the $23b_2$ and 33e orbitals in D_{2d} and the $38a_1$ and 42e orbitals in C_{3v} symmetry. HOMO1 and HOMO2 are shown for the case of D_{2d} symmetry in Figure 4.

We have examined the singlet states in which the nondegenerate orbital arising from the splitting of either HOMO1 or HOMO2 is doubly occupied, and also the triplet states in which the last two electrons are unpaired in the components of the degenerate (e) orbital in both D_{2d} and C_{3v} symmetry. The triplet states are higher in energy than the singlet states for a given choice of HOMO. For example, in D_{2d} symmetry at the MP2-(80e)//HF/6-31G(d) level, the triplets are 15.6 and 3.7 kcal/mol higher than the singlets for HOMO1 and HOMO2, respectively. Therefore, in the following discussion we focus exclusively on the singlet states.

First, we optimized the structures at the HF/6-31G(d) level in both D_{2d} and C_{3v} symmetry for both choices of HOMO. Then various types of post-HF (CI, QCISD, MPn) single-point calculations were carried out at the optimal geometries. Table 2 lists the optimized parameters for all of the states considered in D_{2d}, C_{3v}, and T_d symmetry. As can be seen, there are a total of 60 chemical bonds in each of these symmetries: 6 C−C bonds, 36 Ti−C bonds (12 for outer Ti and 24 for inner Ti), and 18 Ti−Ti bonds (6 for inner−inner Ti and 12 for outer−inner Ti). At all levels of theory, the C−C bond is much like a triple bond. The Ti−C bond between outer Ti atoms and C is considerably shorter than that between inner Ti atoms and C.

Table 3 lists the relative energies for the configurations and states in D_{2d} and C_{3v} symmetry and also the lowest state in T_d symmetry (the closed-shell $^1A_1(5a_1)$ state) at different levels of theory based on the HF optimized geometry. At the HF level,

TABLE 2: Optimized Bond Distances (in Å) for Various States of Ti_8C_{12} in T_d, D_{2d}, and C_{3v} Symmetry from HF, B3LYP, and MP2 Calculations with the 6-31G(d) Basis Set

	T_d					D_{2d}		C_{3v}	
	$^5A_1$ ($7t_2$)	$^5A_1$ ($4t_1$)	$^1A_1$ ($5a_1$)	cusp 1	cusp 2	HOMO1	HOMO2	HOMO1	HOMO2
R(C−C) [6][a]	1.328	1.336	1.309[b]	1.324	1.317	1.335[4][a], 1.318[2][a]	1.313[4], 1.333[2]	1.310[3], 1.352[3]	1.313[3], 1.321[3]
			1.331[c]			1.343[4], 1.345[2]	1.335[4], 1.348[2]	1.332[3], 1.355[3]	1.344[3], 1.333[3]
			1.356[d]	1.342	1.342	1.333[4], 1.340[2]	1.339[4], 1.343[2]	1.332[3], 1.328[3]	1.347[3], 1.335[3]
R(Ti^i−Ti^i) [6][a]	3.133	3.053	2.903[b]	2.902	2.840	2.870[2], 2.927[4]	2.691[2], 2.900[4]	2.884[3], 2.924[3]	3.048[3], 2.764[3]
			2.918[c]			2.871[2], 2.960[4]	2.731[2], 2.885[4]	2.888[3], 2.968[3]	2.907[3], 2.709[3]
			2.957[d]	3.148	2.992	3.001[2], 3.060[4]	2.970[2], 2.995[4]	2.996[3], 3.028[3]	2.745[3], 2.751[3]
R(Ti°−Ti^i) [12][a]	2.935	2.870	2.893[b]	2.850	2.867	2.841[8], 2.874[4]	2.799[8], 3.032[4]	2.859[3], 2.867[6], 2.807[3]	2.844[3], 2.866[6], 2.966[3]
			2.877[c]			2.861[8], 2.932[4]	2.849[8], 3.008[4]	2.916[3], 2.887[6], 2.847[3]	2.930[3], 2.867[6], 2.928[3]
			2.845[d]	3.145	2.925	2.997[8], 3.042[4]	3.021[8], 3.007[4]	3.030[3], 3.012[6], 3.034[3]	3.243[3], 2.905[6], 2.886[3]
R(Ti°−C) [12][a]	1.954	1.916	1.967[b]	1.939	1.940	1.967[4], 1.912[8]	1.970[8], 1.949[4]	1.949[3], 1.899[6], 1.980[3]	1.955[3], 1.964[6], 1.950[3]
			1.963[c]			1.949[4], 1.928[8]	1.957[8], 1.956[4]	1.938[3], 1.921[6], 1.957[3]	1.957[3], 1.951[6], 1.967[3]
			1.969[d]	2.099	2.021	2.016[4], 2.006[8]	2.008[8], 2.025[4]	1.976[3], 2.040[6], 2.036[3]	2.075[3], 2.003[6], 2.101[3]
R(Ti^i−C) [24][a]	2.250	2.235	2.229[b]	2.240	2.208	2.224[8], 2.234[8]	2.215[8], 2.193[8]	2.252[6], 2.239[6], 2.224[6]	2.303[6], 2.225[6], 2.222[6]
						2.235[8]	2.291(8)	2.219[6]	2.216[6]
			2.217[c]			2.198[8], 2.224[8]	2.200[8], 2.193[8]	2.251[6], 2.225[6], 2.220[6]	2.226[6], 2.188[6], 2.230[6]
						2.256[8]	2.263(8)	2.203[6]	2.240[6]
						2.221[8], 2.240[8]	2.185[8], 2.258[8]	2.264[6], 2.229[6], 2.259[6]	2.171[6], 2.154[6], 2.329[6]
			2.202 [d]	2.287	2.260	2.273[8]	2.265[8]	2.220[6]	2.398[6]

[a] The number in square brackets denotes the number of bonds of each type. [b] HF/6-31G(d) optimal geometries. [c] B3LYP/6-31G(d) optimal geometries. [d] MP2(80e)/6-31G(d) optimal geometries.

TABLE 3: Absolute (in hartree) and Relative Energies (in kcal/mol) for States of Ti_8C_{12} in D_{2d}, C_{3v}, and T_d Symmetry Calculated with Different High-Level ab Initio Theories Based on HF/6-31g(d) Optimal Geometries[a]

	D_{2d}		C_{3v}		T_d	
methods	HOMO1	HOMO2	HOMO1	HOMO2	$^1A_1(5a_1)$	absolute energies[b]
HF (optimum)	16.8	12.8	9.3	**0.0**	38.2	−7240.759017
CISD [20e]	24.4	**0.0**	19.5	9.7	32.1	−7241.212049
MP2 [20e]	29.3	**0.0**	35.8	36.2	16.0	−7241.537995
MP4(SDQ) [20e]	13.9	**0.0**	18.7	17.0	30.0	−7241.443387
QCISD [20e]	25.6	**0.0**	23.2	NC	28.2	−7241.408209
CISD [32e]	12.1	**0.0**				−7241.405086
MP4(SDQ) [32e]	0.7	**0.0**				−7241.817694
MP2 [80e]	**0.0**	0.2	14.1	53.2	14.9	−7244.026530
MP4(SDQ) [80e]	**0.0**	37.9	25.2	75.8	24.0	−7243.952698
MP4(SDTQ) [80e]	**0.0**	104.8				−7245.081483
QCISD [80e]	**0.0**	2.7			18.6	−7243.579740

[a] State energies relative to the lowest-energy state at each level of theory. [b] Absolute energies for the lowest state at each level of theory.

the C_{3v} structure with HOMO2 was the lowest-energy one. However, once electron correlation is considered, a D_{2d} structure becomes lower than any C_{3v} structure. The remaining question is at different levels of electron correlation (i.e., the number of electrons correlated) in D_{2d} symmetry, which configuration (HOMO1 or HOMO2) has the lower energy. The configuration with HOMO2 is found to be lower in energy at the HF and the 20-active-electron CISD, MP2, MP4, and QCISD levels of theory, but the configuration with HOMO1 is lower at the 80-active-electron MP2, MP4, and QCISD levels. Again, the correlation of the 60 inner-valance electrons drastically changes the results. Nonperturbative CISD calculations involving 32 (the maximum number of active orbitals allowed by the MOLPRO 2002 program is 16) as well as 20 active electrons are consistent with the same trend, as are MP4 calculations with 20 and 32 active electrons. The energy differences between the two configurations in D_{2d} symmetry are quite different even for 80 active electrons at different levels of theory. The configuration with HOMO1 is only slightly lower than the configuration with HOMO2 at the MP2 and QCISD levels (by 0.2 and 2.7 kcal/mol, respectively) but is lower by 37.9 kcal/mol at the MP4(SDQ) level. At the MP4(SDTQ) level that includes the contributions from triple excitations, the HOMO1 configuration is lower than that with HOMO2 by 104.8 kcal/mol! It would appear that triple and quadruple excitations greatly favor the configuration with HOMO1.

To determine the effect of the basis set on this trend, we extended our calculations for these two configurations in D_{2d}

TABLE 4: Relative Energies of the Two Configurations in D_{2d} Symmetry Calculated with the Wachters(spd)+Bauschlicher(f) Basis for Ti, the cc-pVTZ(spd) Basis for C, and the 6-31G(d) Basis for Both Ti and C[a,b]

	Wachters+f, Ti; VTZ(spd), C			6-31G(d)		
	HOMO1	HOMO2	energies[c]	HOMO1	HOMO2	energies[c]
HF	3.8	0.0	−7241.245123	4.0	0.0	−7240.738730
MP2 [20e]	31.2	0.0	−7242.098900	29.3	0.0	−7241.537995
MP4(SDQ) [20e]	15.3	0.0	−7241.984190	13.9	0.0	−7241.443387
MP2 [80e]	2.0	0.0	−7244.916460	0.0	0.2	−7244.026530
MP4(SDQ) [80e]	0.0	36.2	−7244.785690	0.0	37.9	−7243.952698

[a] All calculations are based on the optimal geometry obtained with the basis set used. [b] State energies relative to the lowest-energy state at each level of theory. [c] Absolute energies for the lowest state at each level of theory.

TABLE 5: Absolute (in hartree) and Relative Energies (in kcal/mol) Calculated with Different High-Level ab Initio Theories Based on the MP2 and B3LYP DFT Optimal Geometry in D_{2d}, C_{3v}, and T_d Symmetry[a]

	D_{2d}		C_{3v}			T_d	
	HOMO1	HOMO2	HOMO1	HOMO2	C_1	$^1A_1(5a_1)$	absolute energies[b]
MP2/6-31G(d) (optimal) [80e]	17.3	0.0	29.2	40.8		46.8	−7244.100273
MP4(SDQ) [80e][c]	**0.0**	43.0				103.1	−7244.120890
QCISD [80e][c]	**0.0**	15.5				15.2	−7243.572060
B3LYP/6-31G(d) (optimal)	1.6	0.7	2.2	1.1	**0.0**	25.5	−7252.671561
MP2 [80e][c]	5.6	**0.0**	20.0	45.5	2.5	22.5	−7244.054721
MP4(SDQ) [80e][c]	**0.0**	35.4			10.5		−7243.982794
B3LYP/sbkjc, vdz (optimal)[d]	3.8	0.9	4.1	0.5	**0.0**	24.7	−921.690498
MP2 [80e][c]	**0.0**	1.1	11.3	43.9	46.3	22.4	−918.996128
B3LYP/ecp10mdf, vtz (optimal)[e]	3.7	0.8	3.8	0.4	**0.0**	23.8	−924.126086
MP2 [80e][c]	5.8	**0.0**	27.2	52.6	55.5	27.9	−921.866399
MP4(SDQ) [80e][c]	**0.0**	36.2					−919.647743

[a] State energies relative to the lowest-energy state at each level of theory. [b] Absolute energies for the lowest state at each level of theory. [c] Ab initio single-point calculations at the corresponding optimized geometries. [d] Pseudopotential basis SBKJC for Ti and the Dunning cc-pVDZ basis for C. [e] Pseudopotential basis ECP10MDF for Ti and the Dunning cc-pVTZ(spd) basis for C.

symmetry using a larger basis set (i.e., the Wachters-(spd)+Bauschlicher(f) basis for Ti[41−43] and the Dunning cc-pVTZ(spd) basis for C[44]). First, the geometries for these two configurations in D_{2d} symmetry were optimized at the HF level using this larger basis. The rms deviation of the 60 chemical bond lengths was used as a measure of the difference between the optimal geometries obtained with the two basis sets (i.e., 6-31G(d) and Wachters+f/cc-pVTZ(spd)). The rms deviation between the calculations with the HOMO1 configuration was 0.0076 Å; that with the HOMO2 configuration was 0.0093 Å. The very small values of these rms deviations indicate that the geometries obtained with these two basis sets are very similar. Second, at the geometries obtained with the larger basis set, single-point calculations were performed at the MP2 and MP4 levels of theory with 20 and 80 valence electrons correlated. The results are collected in Table 4. The results with the larger basis set are clearly consistent with those from the 6-31G(d) basis. At the MP4 level with all-valence electron correlation, the configuration with HOMO1 in D_{2d} symmetry is still lower by 36.2 kcal/mol.

Could the geometry obtained at the HF level of theory be sufficiently inaccurate to be responsible for this dramatic dependence on electron correlation and level of theory? To explore the electron correlation effect on the structure, we also optimized the structures at the MP2 level with all 80 valence electrons correlated. (See Table 2 for optimized parameters.) At the MP2 optimal geometry, higher levels of theory such as MP4 and QCISD with all 80 valence electrons correlated show that the configuration in D_{2d} symmetry with HOMO1 is still lower in energy. The energy difference at the MP4(SDQ) level is 43.0 kcal/mol, somewhat larger than the result obtained at the HF-optimized geometries with the 6-31G(d) basis (37.9 kcal/mol), as seen in Tables 3 and 5. At the QCISD level, the difference is 15.5 kcal/mol, larger than the value of 2.7 kcal/mol obtained at the HF/6-31G(d) optimized geometry. Basically, the high-level calculations based on the HF optimal geometryare consistent with the results based on the MP2 optimal geometry.

As can be seen from the above results, the correlation of only the 20 (metal) outer-valence electrons is not enough, even qualitatively, to account for the electron correlation effect. The correlation of the inner-valence electrons plays an important role in determining the ground state of Ti_8C_{12}. Table 6 lists the correlation energies of both outer- and inner-valence electrons for the two configurations in D_{2d} symmetry. Obviously, the configuration with HOMO2 has more outer-valence-electron correlation energy than the configuration with HOMO1. However, the configuration with HOMO1 has more inner-valence-electron correlation energy, and the difference between these two configurations for the inner-valence-electron case is larger than that for the outer-valence electrons. It seems reasonable that the configuration with HOMO1 would benefit more from correlating the inner-valence electrons; HOMO1 involves CC π^* back-donation interactions with the outer Ti atoms, and the inner-valence orbitals are all associated with CC bonding. HOMO2, however, consists of pure d_{z^2} orbitals on inner Ti atoms, and the configuration with it as HOMO would not be expected to be stabilized as much by correlating the inner-valence electrons.

We had to employ very high level ab initio calculations, such as MP4(SDQ) and QCISD with all valence electrons correlated, to obtain consistent results. However, such high-level calculations are very computationally demanding and are not practical for still larger systems. Suppose for some larger system there were two or more competing configurations for the electronic ground state and that it was not practical to carry out exact CI calculations (e.g., CISD, correlating more than 32 electrons). Would it be possible to employ a rather low-level post-HF method such as MP2 to estimate the difference in inner-valence correlation energies among the competing states reliably? To

TABLE 6: Absolute and Relative Outer- and Inner-valence Electron Correlation Energies and the Energy Difference between the Configurations with HOMO1 and HOMO2 in D_{2d} Symmetry Calculated with Various ab Initio Methods Using the 6-31G(d) Basis

	HF optimal geometries			MP2 optimal geometries	
outer-valence electron (highest 20) correlation energies (in hartree)					
	MP2	MP4(SDQ)	QCISD	MP4(SDQ)	QCISD
HOMO1	−0.759042	−0.688875	−0.635013	−0.792610	−0.683154
HOMO2	−0.799265	−0.704657	−0.669479	−0.769299	−0.713559
ΔE_{OV} (HOMO1 − HOMO2)[a]	+0.040223	+0.015782	+0.034466	−0.023311	+0.030405
inner-valence electron (lowest 60) correlation energies (in hartree)					
	MP2	MP4(SDQ)	QCISD	MP4(SDQ)	QCISD
HOMO1	−2.535186	−2.531521	−2.212412	−2.671075	−2.231700
HOMO2	−2.488255	−2.448833	−2.167184	−2.627201	−2.177860
ΔE_{IV} (HOMO1 − HOMO2)[b]	−0.046931	−0.082688	−0.045228	−0.043874	−0.053840
energy difference between the two configurations (HOMO1 − HOMO2) (in kcal/mol)					
	HF optimal geometries			MP2 optimal geometries	
	MP4(SDQ)	QCISD	CISD	MP4(SDQ)	QCISD	CISD
(20e) + ΔE_{IV}[c]	−15.5	−3.8	−11.5	−44.9	−12.0	−20.8
80e[d]	−38.0	−2.7	N/A	−43.0	−15.5	N/A

[a] ΔE_{OV} (HOMO1 − HOMO2) denotes the difference in outer-valence electron correlation energies between two configurations. [b] ΔE_{IV} (HOMO1 − HOMO2) denotes the difference in inner-valence electron correlation energies between two configurations. [c] Scheme to simulate the results with high-level ab initio methods with all valence electrons correlated: sum of the outer-20 valence electrons' correlation energy calculated at the MP4(SDQ), QCISD, and CISD levels and the inner-valence electron correlation energy calculated at the MP2 level with HF optimal geometries. [d] Results obtained with full-valence electron (80e) correlation.

explore this question, we took the two competing configurations in D_{2d} symmetry as examples. As can be seen from Table 6, the difference in inner-valence correlation energies (i.e., the difference in correlation energy with 80 and 20 active electrons) between these two configurations, ΔE_{IV}(HOMO1 − HOMO2), at different levels of theory is nearly constant. The one exception is the result calculated at the MP4(SDQ) level of theory based on the HF optimal geometry, and this result favors HOMO1 even more than the other methods do. We now use the least computationally demanding (MP2) method to estimate this difference for each configuration. The value obtained (ΔE_{IV} = −0.046931 hartree) was then simply added to the results calculated at MP4, CISD, and QCISD levels with only the outer-20 valence electrons correlated. We can see from Table 6 that the results agree, at least qualitatively, with the results obtained with full-valence electron correlation.

Do DFT methods predict the same result as ab initio methods? We optimized the geometry in the various symmetries with the B3LYP hybrid DFT method using three basis sets: the all-electron 6-31G(d) basis for both Ti and C atoms, the effective core potential SBKJC basis[45] for Ti and the Dunning cc-pVDZ basis[44] for C, and the Stuttgart ECP10MDF basis[46] for Ti and the Dunning cc-pVTZ(spd) basis[44] for C. The B3LYP calculations, like those with the RPBE[47] DFT method,[31] adopt the HOMO2 configuration, seem to prefer lower-symmetry structures, and tend to predict imaginary vibrational frequencies for the higher-symmetry D_{2d} and C_{3v} structures (vide infra). We reoptimized the geometry without any symmetry constraint and obtained a structure with C_1 symmetry and no imaginary frequencies. The potential energy surface near the equilibrium geometry appears to be relatively flat at the B3LYP DFT level of theory. The optimal C_1 structure is only slightly lower than those of D_{2d} and C_{3v} symmetry (Table 5). However, ab initio post-HF calculations (MP4(SDQ) with full-valence-electron correlation) at the preferred DFT geometries indicate that the lower-symmetry structure is 10.5 kcal/mol higher in energy than the D_{2d} structure with the HOMO1 configuration (Table 5).

The results of Baruah et al. with the PBE[48] DFT method[30] are in qualitative agreement with our B3LYP results with ECP basis sets in identifying the T_d, D_{2d}, and C_{3v} structures as low-energy conformations. If the C_1 result in Table 5 is ignored, then our C_{3v} structure has the lowest energy in the calculations with the ECP basis sets for Ti. The fact that Baruah et al. obtained a minimum 0.01 eV lower in energy than their C_{3v} structure is also consistent with our finding a minimum-energy structure in C_1 symmetry that is 0.02 eV lower than the C_{3v} structure.

Some insight into the question of why the post-HF ab initio and DFT results are so different may be offered by the facts that the HOMO−LUMO gaps of the Ti_8C_{12} singlet states are rather small (e.g., 3.8 and 3.2 eV for the D_{2d} structure with HOMO1 at the HF and MP2 levels, respectively) and that there are very low lying triplet states (vide supra). These conditions are often indicators of substantial open-shell character in singlet states. The CI-correlated ab initio methods are more likely to account for such character than DFT methods, which are not ideally suited for treating open-shell (i.e., multiconfigurational) singlet states. Additional support for this notion of open-shell singlet character is provided by the fact that, in our previous RPBE DFT study of singlet states of Ti_8C_{12},[31] we found that spin-polarized calculations in D_{2d} symmetry resulted in a $^3B_1$ state in which the two extra α-spin electrons occupied the $7b_2$ and $4a_2$ orbitals that arise, respectively, from the $4t_1$ and $7t_2$ orbitals in T_d symmetry. Consequently, we reported only spin-unpolarized results.

We explored the question of whether there is a low-energy C_1-symmetry structure at the HF level of theory by reoptimizing the geometry at the HF/6-31G(d) level without any symmetry constraint starting with a C_1-symmetry initial geometry obtained by randomly perturbing the optimal D_{2d} structure. This led to a C_{3v} structure and is consistent with the C_{3v} structures in Table 3 having the lowest energy at the HF level. This result at the ab initio HF level of theory, unlike that using the B3LYP DFT method, implies that Ti_8C_{12} does indeed have some symmetry.

How different are the structures obtained with the different methods? We used the rms deviation of the 60 chemical bond lengths as a measure of the difference between two structures. In a given symmetry, we can thereby characterize the difference in the optimal structures obtained with different methods by a single parameter. In D_{2d} symmetry with the 6-31G(d) basis, the rms deviations between HF-DFT, HF-MP2, and DFT-MP2 optimized structures are 0.024, 0.092, and 0.076 Å, respectively, for the HOMO1 configuration and 0.025, 0.106, and 0.089 Å, respectively, for the HOMO2 configuration. For C_{3v} symmetry, the rms deviations between HF-DFT, HF-MP2, and DFT-MP2 are 0.023, 0.098, and 0.082 Å with HOMO1. The optimal geometries at the HF and B3LYP DFT levels of theory are relatively similar by this criterion, whereas these two differ considerably from the MP2 result. The largest difference in all cases is between the HF and MP2 treatments.

On the basis of all of our calculations regarding geometry and energy, we predict that the D_{2d} (near-T_d) structure with HOMO1 is the energetically lowest structure. At the QCISD-(80e)/6-31G(d)//HF/6-31G(d) level of theory, the energy difference between the optimal D_{2d} (near-T_d) structure and the optimal cusp 1 state is only −1.12 kcal/mol. This energy difference corresponds to the stabilization arising from the geometric distortion part of the Jahn−Teller effect. An estimate of the total (electronic and geometric) stabilization from the Jahn−Teller effect can be obtained by comparing the energies of the optimal D_{2d} (near-T_d) structure and the lowest-energy symmetry-preserving state in T_d symmetry, $^1A_1(5a_1)$. As seen in Table 5, the QCISD(80e)/6-31G(d)//MP2(80e)/6-31G(d) level of theory predicts that the optimal D_{2d} (near-T_d) structure lies 15.2 kcal/mol below the $^1A_1(5a_1)$ state. The MP4(SDQ)(80e)/6-31G(d)//MP2(80e)/6-31G(d) result predicts a much larger total stabilization. The rms deviations of the 60 chemical bond lengths between the T_d and D_{2d} (near-T_d) structures are 0.031 Å (HF) and 0.072 Å (MP2), indicating that the stabilization is accompanied by only a moderate structural distortion.

It is ironic that if one performs an HF/6-31G(d) calculation using a Hückel guess and the Aufbau principle for the orbitals and their occupation then one obtains a structure very similar to our best result (the same symmetry (D_{2d}) and HOMO (HOMO1) and with an rms deviation of 0.092 Å in bond lengths). Intermediate levels of theory appear to provide misleading results, and it takes a very high level of theory to demonstrate that the simplest level of ab initio theory is essentially correct. All of the discussions below regarding the properties and reactivity of Ti_8C_{12} are based on this HF structure. It should be noted that the dipole moment for the optimal D_{2d} (near-T_d) structure is zero by symmetry but there are fairly large dipole moments for the two structures in C_{3v} symmetry, 3.9 and 2.9 D for HOMO1 and HOMO2, respectively. An experimental measurement of the dipole moment would therefore be helpful in confirming our prediction of D_{2d} over C_{3v} as the preferred symmetry.

***T_h* Symmetry.** The fullerene-like cage structure (pentagonal dodecahedron) with T_h symmetry shown in Figure 1 was originally proposed by Castleman and co-workers for Ti_8C_{12},[1−3] and some theoretical work has been carried out for this structure. Both the open-shell nonet state ^9A_g,[17] which is symmetry-preserving, and the open-shell triplet state ^3T_g,[14] which would lead to a Jahn−Teller distortion, have been proposed as the energetically favored state. We optimized various configurations at the HF level, followed by an MP2 calculation with full-valence electron correlation. The closed-shell ^1A_g state having an orbital configuration of $(3a_g)^2(2a_u)^2(3e_g)^4(1e_u)^4(5t_g)^6(4t_u)$,[6] which is not subject to a Jahn−Teller distortion, was found to be the energetically lowest state. However, a frequency calculation at the HF/6-31G(d) level of theory indicated that this structure is highly unstable, having 11 imaginary frequencies. At the MP2/6-31G(d)//HF/6-31G(d) level of theory, the D_{2d} (near-T_d) structure is 322.9 kcal/mol lower than the T_h ^1A_g structure.

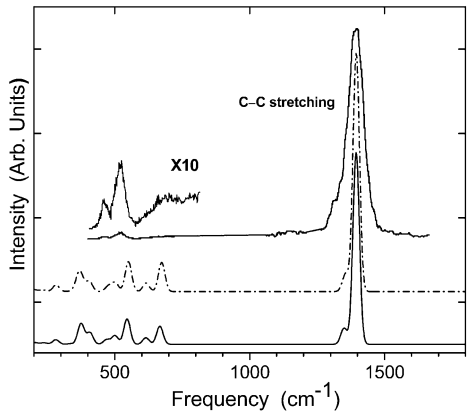

Figure 5. Comparison between the calculated and experimental IR spectrum for Ti_8C_{12}. The upper trace is the experimental spectrum. The middle trace (- · -) was obtained at the HF/6-31G(d) level and scaled by 0.8447. The lower trace was calculated at the HF level with the Wachters(spd)+Bauschlicher(f) basis for Ti and the Dunning cc-pVTZ-(spd) for C and was scaled by 0.8536. Both calculated IR spectra are convoluted with a Gaussian broadening function with a σ of 12 cm^{-1}.

III. Vibrational Frequencies, Electronic Properties, and Reactivity of Ti_8C_{12}

Vibrational Frequencies and IR Spectrum. The harmonic vibrational frequencies of the D_{2d} (near-T_d)-symmetry structure with HOMO1 were calculated at the HF level with the 6-31G-(d) basis set and also the larger basis consisting of the Wachters-(spd)+Bauschlicher(f) for Ti and the Dunning cc-pVTZ(spd) for C. All of the frequencies are real with these two basis sets, indicating that this structure is a true minimum. Figure 5 shows our calculated IR spectra convoluted with a Gaussian broadening function with a σ of 12 cm^{-1}. The simulated spectra resulting from both basis sets are seen to agree quite well (vide infra). The strongest peak corresponds to the doubly degenerate (E) C−C stretching mode associated with the four equivalent C−C bonds in this symmetry. The small shoulder on the low-frequency side of this peak is another C−C stretching mode (a nondegenerate one of B_2 symmetry) associated with the other two equivalent C−C bonds.

It is well known that ab initio harmonic vibrational frequencies are typically larger than the experimentally observed fundamentals[49] mainly because of the neglect of anharmonicity effects as well as the incomplete incorporation of electron correlation and the use of finite basis sets. This overestimation is relatively uniform from system to system; therefore, generic frequency scaling factors can be applied to obtain good agreement between the scaled theoretical harmonic frequencies and the anharmonic experimental frequencies. To obtain agreement between the calculated and experimental large C−C stretching peaks at 1395 cm^{-1},[12] we scaled the computed frequencies in Figure 5 by 0.8447 and 0.8536, respectively, for the small and large basis sets. The scaling factors we used here are smaller than the widely used frequency scaling factor of 0.8928 for the HF/6-31G(d) level of theory.[50,51] This scaling has no effect on the overall shapes of the spectra, which also show good agreement between our calculations and experiment.[12]

TABLE 7: Absolute Energies (in hartree), Number of Imaginary Frequencies, and Unscaled Frequency Range (in cm^{-1}) for Ti_8C_{12} with the HOMO1 Configuration in D_{2d} Symmetry Calculated at the HF Level with Various Basis Sets

basis set	orbitals/ primitives	optimized energy	no. imaginary frequencies	frequency range
6-31G(d)	440/1168	−7240.732315	0	173−1676
6-31+G	468/1168	−7240.624140	0	153−1639
6-31G(d) (Ti), 6-31+G(d)(C)	488/1216	−7240.758367	0	167−1675
TZVP	524/1164	−7241.320790	2 [214i (E)][a]	191−1672
6-31+G(d)	584/1320	−7240.806743	0	165−1670
6-311G(d) (Ti), 6-311+G(d) (C)	632/1080	−7241.088402	2 [226i (E)][a]	205−1674
Wachters+f (Ti), 6-31+G(d) (C)	640/1288	−7241.134846	0	168−1667
Wachters+f (Ti), 6-311+G(d) (C)	688/1336	−7241.212918	0	170−1654
6-311G(2d)	700/1184	−7241.101968	3 [425i (E), 205i][a]	232−1647
Wachters+f(Ti), pVTZ(spd)(C)	700/1444	−7241.239024	0	171−1650

[a] Imaginary frequencies (in cm^{-1}) in square brackets. "E" denotes a doubly degenerate vibrational mode.

Although our HF simulated spectra for the D_{2d} structure with HOMO1 agree with the experimental one, the HF frequency analysis for the C_{3v} structure with HOMO1 yields a rather large (860i cm^{-1}, unscaled) imaginary frequency and a spectrum in which the C−C stretching region is in qualitative disagreement with experiment. The HF frequency analysis of the D_{2d} structure with HOMO2 yielded no imaginary frequencies, but the C−C stretching peaks are too widely separated and the most intense line in the spectrum is predicted to be a doubly degenerate inner Ti−Ti stretch at 608 cm^{-1} (unscaled). The HF spectral analysis of the C_{3v} structure with HOMO2 yields no imaginary frequencies, but the C−C stretching peaks are predicted to be too widely separated. Finally, the B3LYP spectrum at the optimal B3LYP C_1 geometry, unlike the RPBE DFT result[31] for the analogous C_1 structure, does not agree well with experiment. It exhibits strong peaks at 1428 and 1457 cm^{-1} (partially blended by our broadening function) and at 1511 cm^{-1} (unscaled). This spectrum has the "satellite" peak on the wrong side of the main peak. Only our HF simulated spectra in D_{2d} symmetry are substantially in accord with experiment.

Here it should be noted that certain basis sets, typically those with Pople-type triple-ζ basis sets for the Ti atom, predict that the D_{2d} structure with the HOMO1 configuration has low imaginary frequencies at the HF level, as shown in Table 7. This is not surprising because at the HF level the C_{3v} structure with HOMO2 is predicted to have the lowest energy, as discussed above. The TZVP basis set,[52] which produces two low imaginary frequencies for the D_{2d} (HOMO1) structure, was selected for calculating the frequencies for the C_{3v} (HOMO2) structure, and it yields all real frequencies in excellent agreement with those calculated with the 6-31G(d) basis. Apparently, with some basis sets the D_{2d} structure is a stationary point but not a local minimum at the HF level, but this does not necessarily imply that the true minimum corresponds to a low-symmetry (e.g., C_1) structure.

We should mention here the previous DFT calculations that focused on comparing the IR spectra of optimized geometrical structures in various symmetries.[29−31] Although Gueorguiev and Pacheco[29] were the first to attempt to characterize the structure of Ti_8C_{12} by some computed property other than the electronic energy, there are some perplexing aspects of their large-basis, spin-unpolarized, GGA results. Not the least of these is why their T_h structure has more than one C−C stretching peak when all of the C_2 units should be equivalent. This result implies a symmetry-breaking wave function. The IR spectrum of the ^1A_g state we obtained in T_h symmetry exhibits a single C−C stretching peak at 1541 cm^{-1} (unscaled). Similarly, their T_d spectrum apparently corresponds to one of our cusp states, and their T_d* spectrum (based on the authors' "triaxial" description of the deformation from T_d symmetry), to one of our C_{3v} or C_1 states. Our scaled spectra shown in Figure 5 clearly show that the Gueorguiev and Pacheco D_{2d}* state (near the D_{2d} conformer of Rohmer et al.[18]) is not unique in reproducing the experimental line shape. The simulated spectra of the PBE DFT calculated D_{2d} and C_{3v} symmetry structures of Baruah et al.[30] and the RPBE DFT calculated C_1 symmetry structure obtained by Liu et al.[31] also illustrate this point. Finally, the suggestion by Gueorguiev and Pacheco that the experimental spectrum could be explained by the entire population of Ti_8C_{12} molecules formed in the source being in a conformer (their D_{2d}* state) that lies 1.81 eV above the ground-state configuration seems implausible.

Charge Distribution. The CHELPG (**ch**arges from **el**ectrostatic **p**otentials using a **g**rid-based method) scheme by Breneman and Wiberg[53] was used to calculate the charge distribution of Ti_8C_{12}. The basic idea of this method is that the atomic charges are fitted to reproduce the molecular electrostatic potential (MEP) at a number of points around the molecule. The calculations show that all of the C atoms are negatively charged (−0.66e for the C atoms in the four equivalent C_2 units and −0.62e for the C atoms in the other two equivalent C_2 units) and that all of the Ti atoms are positively charged (0.89e for outer Ti and 1.05e for inner Ti). Obviously, there is electron transfer from Ti (both outer and inner Ti atoms) to C, and the inner Ti atoms donate more electron density than the outer ones. As mentioned above, the first 30 valence orbitals of Ti_8C_{12} fall into 5 groups of 6 orbitals corresponding to each of the first 5 N_2-like occupied valence orbitals of the building block fragment TiC_2 (Figure 2).[39] The building block TiC_2 is more associated with an inner Ti atom, which is η^2-bonded to three C_2 units. Therefore, as in TiC_2, we suppose that there are two electrons transferred from each inner Ti atom to a C_2 unit and that the formal oxidation state for inner Ti is Ti(II). The outer Ti atoms are σ-bonded to C atoms, and one electron is supposed to be transferred from each outer Ti atom to a C atom, just as in the building block TiC.[54] Therefore, the formal oxidation state for outer Ti is Ti(I). Our assignments of formal oxidation states for the Ti atoms are different than in Rohmer et al.'s work[21] in which the Ti(0) and Ti(III) formal oxidation states were assigned for outer and inner Ti atoms, respectively. Their assignment, however, was based on the open-shell $^5A_1(7t_2)$ state.

Orbital Properties. The lowest unoccupied molecular orbital (LUMO) is a d_{z^2}-like orbital on the outer Ti atoms, with a large lobe projecting out into the vacuum (Figure 4). We would therefore expect Ti_8C_{12} to act as a Lewis acid, an acceptor of a lone pair of electrons, and to interact with a Lewis base such as H_2O or NH_3. In the case of CO, we would expect a competition between σ donation and π back-donation interactions with a Ti atom. Second, all of the Ti atoms are positively charged (which should enhance the Lewis acid activity), and the C atoms are negatively charged. There is electron transfer

TABLE 8: Bonding Distance (in Å), Binding Energy, BE (in kcal/mol), and Charge on the Adducts for the Reactions of Ti_8C_{12} with H_2O, Cl, and CO[a]

adduct	sites	R(Ti−L)	total BE[b] HF	total BE[b] MP2[c]	ave BE per adduct HF	ave BE per adduct MP2[c]	charge (on each adduct)
H_2O	Ti° [4][d]	2.222	104.1	110.3	26.0	27.6	0.101e
	Ti^i[4][d]	2.212	80.5	90.5	20.1	22.6	0.123e
	Ti° [4] + Ti^i[4][d]	2.217[g], 2.212[h]	77.6	161.0	9.7	20.1	0.108e, 0.118e
Cl	Ti° [4][d]	2.272	375.9	232.4	94.0	58.1	−0.428e
	Ti^i[4][d]	2.301	352.3	308.2	88.1	77.0	−0.435e
	Ti° [4] + Ti^i[4][d]	2.223[g], 2.229[h]	580.8	615.2	72.6	76.9	−0.330e, −0.320e
CO	Ti° [4][d]	2.393	66.4	85.0	16.6	21.2	0.079e
	Ti° [1][e]		11.6	11.0	11.6	11.0	
	Ti^i[4][d]	2.264	−130.8	−451.1	−32.7	−112.8	0.067e
	Ti^i[1][e]		*−234.2*	*−269.6*	*−234.2*	*−269.6*	
	Ti° [4] + Ti^i[4][d]	2.262[g], 2.218[h]	−17.5	−606.3	−2.2	−75.8	0.035e, −0.021e
	Ti° [4] + Ti^i[1][f]		*−6.9*	*−684.0*	*−1.4*	*−136.8*	

[a] Geometries are optimized at the HF/6-31G(d) level of theory within D_{2d} symmetry. [b] Binding energy BE = E(complex) − E(Ti_8C_{12} + adduct). [c] Single-point calculations at the MP2/6-31G(d) level of theory. [d] Ti°[4] denotes the reaction of four adducts added to the four outer Ti atoms; Ti^i[4] denotes the reaction of four adducts added to the four inner Ti atoms; and Ti°[4] + Ti^i[4] denotes the reaction of eight adducts added to both four outer and inner Ti atoms. [e] Ti° [1] and Ti^i[1] denote one CO molecule added to one outer Ti atom and one inner Ti atom, respectively. Geometries are taken from the optimal geometries of the adducts with four CO molecules added. [f] Ti°[4] + Ti^i[1] denotes four CO molecules added to the four outer Ti atoms and one CO added to the one inner Ti atom. The geometry was taken from the optimal geometry of the adducts with eight CO molecules added to all eight Ti atoms. [g] The bond distance between the outer Ti and the adduct. [h] The bond distance between the inner Ti and the adduct.

from Ti to C, just as in the building block TiC_2.[39] As mentioned above, the six C−C units are essentially triple bonded, so the N_2-like C_2 unit can be described as C_2^{2-}. If the species interacting with Ti_8C_{12} has a large electron affinity, such as Cl, there would be competition in obtaining electron density from Ti between the incoming species and the C_2 units. We can therefore anticipate π back-donation from C_2 units through Ti d orbitals to the incoming adduct species. These predictions of the possible reactivity of Ti_8C_{12} toward other molecules on the basis of its electronic properties are consistent with previous experimental[4−7,11] and theoretical[24,25,28,31] studies.

Reactivity toward H_2O, CO, and Cl. There are two sets of Ti atoms (inner and outer), and as indicated in the previous section, they have different charges. Moreover, the lowest unoccupied orbitals on each set of Ti atoms are all d_{z^2}-like orbitals, but the ones on the outer Ti atoms (LUMO) are lower in energy than those on the inner Ti atoms by about 12.4 kcal/mol. These two sets of Ti atoms should correspond to two different reactive sites in the Ti_8C_{12} molecule. Previous theoretical studies of the reactivity of Ti_8C_{12}, mainly the work of Poblet et al.[24] and Liu et al.,[31] have indeed demonstrated this characteristic. In these two studies, the SCF-HF and DFT methods were employed, and the calculations were carried out in T_d and C_1 symmetry, respectively. The present work, however, has demonstrated that (1) high-level ab initio methods predict a D_{2d} symmetry structure to be the most stable geometric structure; (2) proper electron correlation (all valence electrons) is important for the Ti_8C_{12} system; and (3) DFT methods, which employ empirical functionals for the effect of correlation, give somewhat different results than ab initio calculations. Therefore, the reactivity of Ti_8C_{12} was reinvestigated in this work in the proper symmetry and orbital configuration with both HF and post-HF ab initio methods.

In this work, we studied Ti_8C_{12} reactivity toward three different but typical adducts: (1) H_2O and CO, both of which can donate a lone pair of electrons (localized on O and C, respectively), and (2) the Cl atom, which has an unpaired electron and has a very large electron affinity. In addition to donating an electron pair, CO can also accept back-donated electrons in an unoccupied π^* orbital.[55] These three adducts were chosen to study the Lewis acid and the electron-transfer reactivity of Ti_8C_{12}. Three different kinds of adduct scenarios were considered, as in Poblet et al.'s work.[24] With these we seek to elucidate differences in reactivity of the two types of reactive Ti sites: four reactants are added to the outer Ti atoms simultaneously, four are added to the inner Ti atoms simultaneously, and eight are added to all of the Ti atoms. In all of the calculations using these scenarios, the geometry was constrained to D_{2d} symmetry for both Ti_8C_{12} and all adducts.

We optimized the geometries at the HF/6-31G(d) level and followed that by an MP2/6-31G(d) single-point calculation with all valence electrons correlated. Table 8 lists the bonding distances between the various types of Ti atoms and the different adducts, the total and average binding energies, and the net charge on each adduct. The distances between Ti sites and adducts span the range of 2.21−2.22 Å for H_2O, 2.22−2.30 Å for Cl, and 2.22−2.39 Å for CO. These Ti−CO bond lengths are quite long and probably reflect the absence of back-donation from Ti to CO. The size of the adduct complexes is on the nanoscale (e.g., 9.87, 9.47, and 12.12 Å for H_2O, Cl, and CO, respectively). In the interaction between Ti_8C_{12} and H_2O, H_2O is positively charged. The metcar and the adduct H_2O interact through the Lewis acid−base mechanism mentioned above: the lone pair of electrons on the O p_z orbital is partially transferred to an empty Ti d_{z^2} orbital. The addition of H_2O to both the outer and inner sites is highly exothermic. The Cl atom becomes negatively charged through its interaction with Ti_8C_{12}, obviously as the result of electron transfer from Ti_8C_{12} to Cl. The excess electron density on the C_2^{2-} units is partially donated to Cl through the Ti d_{z^2} orbital. This partial charge transfer is accompanied by a large structural change in the metcar, primarily in the bond lengths of the inner Ti tetrahedron that increase by 0.762 Å (4) and 0.575 Å (2). As in the case of H_2O, the addition of Cl to both outer and inner Ti sites is highly exothermic. Interestingly, the addition of four CO molecules to the outer Ti sites is also exothermic, but the addition of CO to the inner sites is highly endothermic (although this adduct complex is calculated to correspond to a stationary point). The addition of eight CO molecules to both outer and inner Ti sites is also endothermic. When only one CO is added to an outer Ti

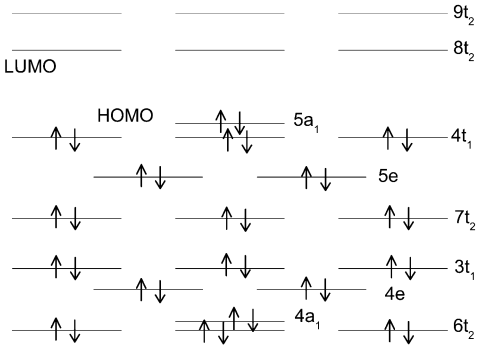

Figure 6. Metal d-orbital energy diagram for Mo_8C_{12} with a tetracapped tetrahedron structure within T_d symmetry calculated at the HF level of theory. Basis sets: ECP28MWB, Mo; cc-pVTZ(spd), C.

atom, the reaction is 11.0 kcal/mol exothermic at the MP2 level. This value is smaller (on a per CO basis) than that for four CO molecules added to the four outer Ti atoms (85.0 kcal/mol) and implies that the adduct complexes become more stable as more CO molecules are added to the outer Ti atoms. The addition of one CO to an inner Ti atom is endothermic by 269.6 kcal/mol. Would this endothermicity be offset by adding four CO molecules to the four outer Ti atoms and only one CO to an inner Ti atom? The answer is no; this process is still highly endothermic (by 684.0 kcal/mol). These results suggest that we should anticipate that only four CO molecules could be added to Ti_8C_{12}. The present results of the reactivity of Ti_8C_{12} are in agreement with the experimentally observed reactivity of Ti_8C_{12} as well as the previous theoretical results.[4−7,11,24,25,28,31]

IV. Geometric Structure and Energetics of Mo_8C_{12}

By analogy to Ti_8C_{12}, we anticipated a similar tetracapped tetrahedron structure for Mo_8C_{12} given the facts that (1) they have the same stoichiometry (magic numbers 8 and 12) and (2) both Mo and Ti are early transition metals. However, because Mo and Ti have different numbers of valence electrons and different electronic ground states, they might behave quite differently. Similar to Ti_8C_{12}, the first 30 valence orbitals are all related to the 6 C_2 units and correspond to the first 5 valence orbitals in MoC_2.[39] That leaves 36 valence electrons that are associated with the metal Mo atoms. Figure 6 shows the metal d-orbital energy diagram obtained at the HF level of theory with the Stuttgart ECP28MWB(spd) basis for Mo[56] and the Dunning cc-pVTZ(spd) basis for C.[44] Here we number the orbitals beginning with the valence shell so that they correspond to those for Ti_8C_{12}. Interestingly, we found that there is no Jahn−Teller effect for the Mo_8C_{12} cluster with a T_d symmetry structure if the electrons are accommodated according to the Aufbau principle. We optimized the geometry within T_d symmetry at both the HF and B3LYP DFT levels. The optimized bond distances are listed in Table 9. Similar to Ti_8C_{12}, there are 60 chemical bonds (6 C−C bonds, 36 Mo−C bonds (12 for outer Mo and 24 for inner Mo), and 18 Mo−Mo bonds (6 for inner−inner Mo, 12 for outer−inner Mo)). The C−C bond is again like a triple bond, and the Mo−C bond between outer Mo atoms and C is considerably shorter than that between inner Mo atoms and C.

The harmonic vibrational frequencies were calculated at the optimal geometry at the HF and B3LYP levels with SBKJC (Mo)[45] and cc-pVDZ (C)[44] basis sets. At the HF level, this structure is a true minimum (all frequencies are real); however, it is not a true minimum at the B3LYP level, which predicts a small triply degenerate imaginary vibrational frequency (296i cm^{-1}). We reoptimized the geometry at the B3LYP level without any symmetry constraint, and this produced a lower-symmetry (near-D_2) structure (in near-D_2 symmetry, the six C_2 units are split into three groups, two in each group). It should be noted that the energy difference between the T_d and near-D_2 structures is very small at the B3LYP level (only 0.5 and 0.4 kcal/mol with the SBKJC/VDZ and ECP28MWB/VTZ basis sets, respectively), even though there is a moderately large structural difference between these two species (rms deviation of 0.05 Å for both basis sets). Again, as in Ti_8C_{12}, the B3LYP DFT method tends to prefer a lower-symmetry structure and predict a relatively flat potential surface near the equilibrium geometry. Single-point HF calculations with the SBKJC/VDZ basis at the B3LYP-optimized T_d and C_1 (near-D_2) geometries showed the T_d structure to lie 71.3 kcal/mol above the C_1 structure, but similar MP2(96e) calculations predicted the T_d structure to lie 344.4 kcal/mol below the C_1 structure.

When the geometries were optimized using the HF method with the SBKJC/VDZ basis, we found that the C_1 optimization converged to a C_s structure with an energy of −163.9 kcal/mol relative to that of the optimal T_d structure. However, MP2(96e) single-point calculations at the two optimal geometries completely reversed the HF result, predicting the C_s structure at +839.2 kcal/mol relative to the T_d structure. Single-point HF and MP2 calculations with the larger ECP28MWB/VTZ basis at the HF/SBKJC,VDZ optimal geometries supported this result, predicting the C_s structure at −142.4 and +871.1 kcal/mol, respectively, relative to the T_d structure. This is a very large correlation energy effect, which may well be exaggerated by the MP2 method, but it seems unlikely that a refined treatment

TABLE 9: Optimized Bond Distances (in Å) for Mo_8C_{12} in T_d and Near-D_2 Symmetry from HF and B3LYP Calculations with Two Basis Sets[a]

parameters	HF (T_d)	B3LYP1 (T_d)	B3LYP (near-D_2)
R(C−C) [6][b]	1.372[c]	1.379	1.343[2][b], 1.382[2], 1.409[2]
	1.365[d]	1.366	1.329[2], 1.368[2], 1.397[2]
R(Mo^i−Mo^i) [6][b]	2.585[c]	2.649	2.619[2], 2.648[2], 2.779[2]
	2.573[d]	2.640	2.610[2], 2.636[2], 2.772[2]
R(Mo°−Mo^i) [12][b]	2.803[c]	2.833	2.726−2.728[4], 2.880−2.883[8]
	2.786[d]	2.817	2.707−2.709[4], 2.865−2.870[8]
R(Mo°−C) [12][b]	1.959[c]	1.975	1.924[4], 1.963[4], 2.040[4]
	1.950[d]	1.969	1.920[4], 1.958[4], 2.032[4]
R(Mo^i−C) [24][b]	2.294[c]	2.307	2.274[4], 2.295[4], 2.304[4], 2.318−2.322[4], 2.339[4], 2.344[4]
	2.284[d]	2.298	2.266[4], 2.286[4], 2.292[4], 2.308−2.314[4], 2.329[4], 2.337[4]

[a] (1) SBKJC basis set for Mo and Dunning cc-pVDZ for C; (2) ECP28MWB basis set for Mo and Dunning cc-pVTZ(spd) for C. [b] The numbers in square brackets denote the number of bonds of each type. [c] Optimal geometries with SBKJC (Mo) and cc-pVDZ (C) basis sets. [d] Optimal geometries with ECP28MWB (Mo) and cc-pVTZ(spd) (C) basis sets.

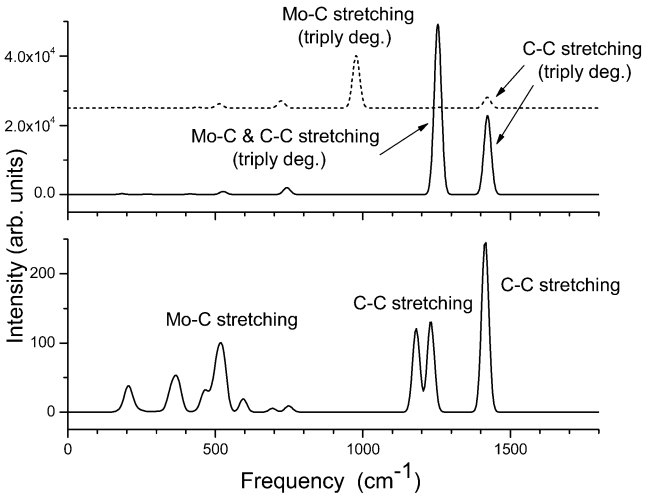

Figure 7. Simulated IR spectrum of Mo_8C_{12}. The upper panel was calculated at the HF level with T_d symmetry using the SBKJC, Mo; cc-pVDZ, C (upper trace) and ECP28MWB, Mo; cc-pVTZ, C (lower trace) basis sets. The lower panel was calculated at the B3LYP DFT level with C_1 (near-D_2) symmetry using the SBKJC, Mo; cc-pVDZ, C basis. Both spectra are convoluted with a Gaussian broadening function with a σ of 12 cm^{-1}.

of the electron correlation would change the qualitative identification of the most stable structure.

Figure 7 shows simulated IR spectra of Mo_8C_{12} convoluted with a Gaussian broadening function with a σ of 12 cm^{-1}. The upper spectra are calculated at the HF level with the SBKJC/VDZ and ECP28MWB/VTZ basis in T_d symmetry; the lower spectrum is calculated at the B3LYP level with the SBKJC/VDZ basis in near-D_2 symmetry. Not only do these two methods yield quite different spectra, but there is a significant basis set effect in the HF spectra. At the HF level, the C−C stretching mode is predicted to be around 1422 cm^{-1} (unscaled) for both basis sets, but there is another stronger peak at 977 cm^{-1} in the SBKJC/VDZ spectrum associated with the triply degenerate Mo−C stretch. With the ECP28MWB/VTZ basis, the Mo−C stretching vibration mixes with the C−C stretch to shift the triply degenerate peak to 1254 cm^{-1}. Other features of the two HF spectra are quite similar. The near-D_2 structure at the B3LYP level is predicted to have three C−C stretching peaks associated with three groups of C_2 units. One of the C−C stretching peaks (the strongest, at ∼1415 cm^{-1}) is quite similar to the one at the HF level, but the Mo−C stretch is shifted down to 528 cm^{-1}.

In Mo_8C_{12}, the Mo atoms are positively charged (0.696e for inner Mo and 0.560e for outer Mo), and the C atoms are negatively charged (−0.419e). These are generally smaller charges than were computed with the same method for Ti_8C_{12}. The LUMO is the empty d_{xz} orbital on outer Mo atoms. On the basis of its geometrical structure and electronic properties, we anticipate that Mo_8C_{12} would have reactivity patterns similar to those in Ti_8C_{12}, but the absolute reactivity of the Mo and Ti sites could be different.

V. Summary and Conclusions

The tetracapped tetrahedron structure with D_{2d} (near-T_d) symmetry is predicted to be the energetically favored geometric structure for Ti_8C_{12} through extensive calculations employing different high-level ab initio methods such as CI, MPn, and QCISD. The different methods were found to yield consistent results at the same level of treatment of electron correlation. The results, however, were found to depend strongly on the level of treatment of electron correlation, and only at the full-valence level of correlation do the results agree with those in which all electrons are correlated. Correlating only the highest 20 electrons, those mostly associated with the metal atoms, does not account for the vast majority of the correlation energy of the valence electrons, and including the correlation of the 60 inner-valence electrons drastically changes the results.

In the D_{2d} structure, the six C_2 units are split into two groups: four in one group and the other two in another group. The eight Ti atoms are also split into two sets: the four equivalent capping Ti atoms and the four equivalent capped atoms. This structure results from the first-order Jahn−Teller distortion of T_d symmetry, and the energy of the Ti_8C_{12} metcar is lowered by 1.12 kcal/mol from that of a T_d cusp state with a symmetry-breaking wave function at the QCISD/6-31G(d)//HF/6-31G(d) level of theory because of this Jahn−Teller distortion. An estimate of 15.2 kcal/mol for the total (electronic and geometric) stabilization from the Jahn−Teller effect was obtained by comparing the energies of the optimal D_{2d} (near-T_d) structure and the lowest-energy symmetry-preserving state in T_d symmetry, $^1A_1(5a_1)$, at the QCISD(80e)/6-31G(d)//MP2-(80e)/6-31G(d) level of theory. The most important feature of this configuration that makes it different from other competing configurations is that the HOMO is composed of the d_{xz} orbitals on the outer Ti atoms interacting with the C−C π^* orbitals.

The properties of Ti_8C_{12} were investigated within the preferred D_{2d} symmetry. The IR spectrum has been simulated, and it agrees well with the experimental one. The Ti atoms are positively charged, and the C atoms are negatively charged. The formal oxidation states for outer and inner Ti atoms are proposed to be Ti(I) and Ti(II), respectively. Ti_8C_{12} is predicted to be a Lewis acid because the LUMO is composed of the empty d_{z^2} orbitals on the positively charged outer Ti atoms with a large lobe projecting out into the vacuum. Thus, the outer and inner Ti atoms are predicted to present two distinct reactive sites, and this was verified by examining the reactivity of Ti_8C_{12} toward the H_2O, Cl, and CO species.

Ti_8C_{12} interacts with H_2O through a Lewis acid−base interaction mechanism, and the addition of H_2O to both outer and inner Ti atoms is highly exothermic. Ti_8C_{12} also undergoes an oxidation reaction with the Cl atom, and excess electron density from the C_2 units is back-donated to Cl through a Ti d_{z^2} orbital. The addition of Cl is a highly exothermic process with both outer and inner Ti sites. For CO, we found that only the addition of four CO molecules to the four outer Ti atom sites is feasible; the addition to the inner Ti sites would be highly endothermic. Our HF and MP2 calculations in D_{2d} symmetry are therefore consistent with previous experimental[4−7,11] and theoretical[24,25,28,31] studies of Ti_8C_{12} reactivity.

A similar tetracapped tetrahedron structure with T_d symmetry for Mo_8C_{12} is not subject to a Jahn−Teller effect at the HF level, but a lower-symmetry (near-D_2) geometry is preferred at the B3LYP DFT level. The simulated IR spectrum at both the HF and B3LYP levels predicts a C−C stretching mode at around 1420 cm^{-1}. Similar to Ti_8C_{12}, the Mo atoms are positively charged, and the C atoms are negatively charged. Mo_8C_{12} is predicted to have qualitatively similar reactivity patterns to those of Ti_8C_{12}, but absolute reactivities of the Mo and Ti species may differ.

The HF and DFT methods predict similar geometrical structures within the same constrained symmetry, and they differ considerably from the MP2-optimized geometry. The B3LYP DFT method tends to prefer lower-symmetry structures and generates a relatively flat potential energy surface. It is suggested that differences between post-HF ab initio and DFT results arise primarily from the open-shell character of the singlet states of the metcars.

Acknowledgment. This work was performed at Brookhaven National Laboratory under contract DE-AC02-98CH10886 with the U.S. Department of Energy and supported by its Division of Chemical Sciences, Office of Basic Energy Sciences. J.T.M. thanks H.-G. Yu and M. Head-Gordon for helpful discussions.

References and Notes

(1) Guo, B. C.; Kerns, K. P.; Castleman, A. W. *Science* **1992**, *255*, 1411.
(2) Guo, B. C.; Wei, P.; Purnell, J.; Buzza, S. A.; Castleman, A. W. *Science* **1992**, *256*, 515.
(3) Wei, P.; Guo, B. C.; Purnell, J.; Buzza, S. A.; Castleman, A. W. *J. Phys. Chem.* **1992**, *96*, 4166.
(4) Guo, B. C.; Kerns, K. P.; Castleman, A. W. *J. Am. Chem. Soc.* **1993**, *115*, 7415.
(5) Deng, H. T.; Guo, B. C.; Kerns, K. P.; Castleman, A. W. *J. Phys. Chem.* **1994**, *98*, 13373.
(6) Kerns, K. P.; Guo, B. C.; Deng, H. T.; Castleman, A. W. *J. Am. Chem. Soc.* **1995**, *117*, 4026.
(7) Deng, H. T.; Kerns, K. P.; Castleman, A. W. *J. Am. Chem. Soc.* **1996**, *118*, 446.
(8) Wang, L. S.; Li, S.; Wu, H. B. *J. Phys. Chem.* **1996**, *100*, 19211.
(9) Sakurai, H.; Castleman, A. W. *J. Phys. Chem. A* **1997**, *101*, 7695.
(10) Li, S.; Wu, H. B.; Wang, L. S. *J. Am. Chem. Soc.* **1997**, *119*, 7417.
(11) Auberry, K. J.; Byun, Y. G.; Jacobson, D. B.; Freiser, B. S. *J. Phys. Chem. A* **1999**, *103*, 9029.
(12) Heijnsbergen, D.; Helden, G.; Duncan, M. A.; Roij, A.; Meijer, G. *Phys. Rev. Lett.* **1999**, *83*, 4983.
(13) Heijnsbergen, D.; Duncan, M. A.; Meijer, G.; Helden, G. v. *Chem. Phys. Lett.* **2001**, *349*, 220.
(14) Rohmer, M. M.; Devaal, P.; Benard, M. *J. Am. Chem. Soc.* **1992**, *114*, 9696.
(15) Reddy, B. V.; Khanna, S. N.; Jena, P. *Science* **1992**, *258*, 1640.
(16) Dance, I. *J. Chem. Soc., Chem. Commun.* **1992**, 1779.
(17) Hay, P. J. *J. Phys. Chem.* **1993**, *97*, 3081.
(18) Rohmer, M. M.; Benard, M.; Henriet, C.; Bo, C.; Poblet, J. M. *J. Chem. Soc., Chem. Commun.* **1993**, 1182.
(19) Chen, H.; Feyereisen, M.; Long, X. P.; Fitzgerald, G. *Phys. Rev. Lett.* **1993**, *71*, 1732.
(20) Reddy, B. V.; Khanna, S. N. *J. Phys. Chem.* **1994**, *98*, 9446.
(21) Rohmer, M. M.; Benard, M.; Bo, C.; Poblet, J. M. *J. Am. Chem. Soc.* **1995**, *117*, 508.
(22) Benard, M.; Rohmer, M. M.; Poblet, J. M.; Bo, C. *J. Phys. Chem.* **1995**, *99*, 16913.
(23) Dance, I. *J. Am. Chem. Soc.* **1996**, *118*, 6309.
(24) Poblet, J. M.; Bo, C.; Rohmer, M. M.; Benard, M. *Chem. Phys. Lett.* **1996**, *260*, 577.
(25) Ge, M. F.; Feng, J. K.; Tian, W. Q.; Li, Z. R.; Huang, X. R.; Sun, C. C. *Chem. Phys. Lett.* **1998**, *282*, 54.
(26) Rohmer, M. M.; Benard, M.; Poblet, J. M. *Chem. Rev.* **2000**, *100*, 495.
(27) Joswig, J. O.; Springborg, M.; Seifert, G. *Phys. Chem. Chem. Phys.* **2001**, *3*, 5130.
(28) Ivanovskii, A. L.; Sofronov, A. A.; Makurin, Y. N. *Russ. J. Coord. Chem.* **2001**, *27*, 23.
(29) Gueorguiev, G. K.; Pacheco, J. M. *Phys. Rev. Lett.* **2002**, *88*, 115504.
(30) Baruah, T.; Pederson, M. R.; Lyn, M. L.; Castleman, A. W. *Phys. Rev. A* **2002**, *66*, 053201.
(31) Liu, P.; Rodriguez, J. A.; Hou, H.; Muckerman, J. T. *J. Chem. Phys.* **2003**, *118*, 7737.
(32) Pilgrim, J. S.; Duncan, M. A. *J. Am. Chem. Soc.* **1993**, *115*, 6958.
(33) Lightstone, J. M.; Mann, H.; Wu, M.; Johnson, P. M.; White, M. G. *J. Phys. Chem. B* **2003**, *107*, 10359.
(34) Lin, Z. Y.; Hall, M. B. *J. Am. Chem. Soc.* **1993**, *115*, 11165.
(35) Rassolov, V.; Pople, J. A.; Ratner, M.; Windus, T. L. *J. Chem. Phys.* **1998**, *109*, 1223.
(36) Hariharan, P. C.; Pople, J. A. *Theor. Chim. Acta* **1973**, *28*, 213.
(37) Frisch, M. J.; Trucks, G. W.; Schlegel, H. B.; Scuseria, G. E.; Robb, M. A.; Cheeseman, J. R.; Zakrzewski, V. G.; Montgomery, J. A., Jr.; Stratmann, R. E.; Burant, J. C.; Dapprich, S.; Millam, J. M.; Daniels, A. D.; Kudin, K. N.; Strain, M. C.; Farkas, O.; Tomasi, J.; Barone, V.; Cossi, M.; Cammi, R.; Mennucci, B.; Pomelli, C.; Adamo, C.; Clifford, S.; Ochterski, J.; Petersson, G. A.; Ayala, P. Y.; Cui, Q.; Morokuma, K.; Malick, D. K.; Rabuck, A. D.; Raghavachari, K.; Foresman, J. B.; Cioslowski, J.; Ortiz, J. V.; Stefanov, B. B.; Liu, G.; Liashenko, A.; Piskorz, P.; Komaromi, I.; Gomperts, R.; Martin, R. L.; Fox, D. J.; Keith, T.; Al-Laham, M. A.; Peng, C. Y.; Nanayakkara, A.; Gonzalez, C.; Challacombe, M.; Gill, P. M. W.; Johnson, B. G.; Chen, W.; Wong, M. W.; Andres, J. L.; Head-Gordon, M.; Replogle, E. S.; Pople, J. A. *Gaussian 98*, revision A.7; Gaussian, Inc.: Pittsburgh, PA, 1998.
(38) Amos, R. D.; Bernhardsson, A.; Berning, A.; Celani, P.; Cooper, D. L.; Deegan, M. J. O.; Dobbyn, A. J.; Eckert, F.; Hampel, C.; Hetzer, G.; Knowles, P. J.; Korona, T.; Lindh, R.; Lloyd, A. W.; McNicholas, S. J.; Manby, F. R.; Meyer, W.; Mura, M. E.; Nicklass, A.; Palmieri, P.; Pitzer, R.; Rauhut G.; Schütz, M.; Schumann, U.; Stoll, H.; Stone, A. J.; Tarroni, R.; Thorsteinsson, T.; Werner, H.-J. *MOLPRO*, a package of ab initio programs designed by Werner, H.-J. and Knowles, P. J.
(39) Hou, H.; Muckerman, J. T. *J. Chem. Phys.*, submitted for publication.
(40) Bunker, P. R.; Jensen, P. *Molecular Symmetry and Spectroscopy*, 2nd ed.; NRC Research Press: Ottawa, Canada, 1998.
(41) Wachters, A. J. H. *J. Chem. Phys.* **1970**, *52*, 1033.
(42) Wachters, A. J. H. *IBM Technol. Rep.* **1969**, RJ584.
(43) Bauschlicher, C. W.; Langhoff, S. R. J.; Barnes, L. A. *J. Chem. Phys.* **1989**, *91*, 2399.
(44) Dunning, T. H. J. *J. Chem. Phys.* **1989**, *90*, 1007.
(45) Stevens, W. J.; Krauss, M.; Basch, H.; Jasien, P. G. *Can. J. Chem.* **1992**, *70*, 612.
(46) Dolg, M.; Wedig, U.; Stoll, H.; Preuss, H. *J. Chem. Phys.* **1987**, *86*, 866.
(47) Hammer, B.; Hansen, L. B.; Nørskov, J. K. *Phys. Rev. B* **1999**, *59*, 7413.
(48) Perdew, J. P.; Burke, K.; Ernzerhof, M. *Phys. Rev. Lett.* **1996**, *77*, 3865.
(49) Hehre, W. J.; Radom, L.; Schleyer, P. v. R.; Pople, J. A. *Ab Initio Molecular Orbital Theory*; Wiley: New York, 1986.
(50) Pople, J. A.; Head-Gordon, M.; Fox, D. J.; Raghavachari, K.; Curtiss, L. A. *J. Chem. Phys.* **1989**, *90*, 5622.
(51) Curtiss, L. A.; Carpenter, J. E.; Raghavachari, K.; Pople, J. A. *J. Chem. Phys.* **1992**, *96*, 9030.
(52) Schaefer, A.; Huber, C.; Ahlrichs, R. *J. Chem. Phys.* **1994**, *100*, 5829.
(53) Breneman, C. M.; Wiberg, K. B. *J. Comput. Chem.* **1990**, *11*, 361.
(54) Poulin, N.; Muckerman, J. T.; Sears, T. J. To be submitted for publication.
(55) Davidson, E. R.; Kunze, K. L.; Machado, F. B. C.; Chakravorty, S. J. *Acc. Chem. Res.* **1993**, *26*, 628.
(56) Andrae, D.; Haeussermann, U.; Dolg, M.; Stoll, H.; Preuss, H. *Theor. Chim. Acta* **1990**, *77*, 123.